Math. Model. Nat. Phenom.
Vol. 2, No. 4, 2007, pp. 135-151

Concentration in the nonlocal Fisher equation: the Hamilton-Jacobi limit

Benoît Perthame[a] **and Stephane Génieys** [b] [1]

[a] Département de Mathématiques et Applications, École Normale Supérieure, CNRS UMR 8553, 45 rue d'Ulm, F 75230 Paris cedex 05
[b] Université de Lyon, Université Lyon1, CNRS UMR 5208 Institut Camille Jordan, F - 69200 Villeurbanne Cedex, France

Abstract. The nonlocal Fisher equation has been proposed as a simple model exhibiting Turing instability and the interpretation refers to adaptive evolution. By analogy with other formalisms used in adaptive dynamics, it is expected that concentration phenomena (like convergence to a sum of Dirac masses) will happen in the limit of small mutations. In the present work we study this asymptotics by using a change of variables that leads to a constrained Hamilton-Jacobi equation. We prove the convergence analytically and illustrate it numerically. We also illustrate numerically how the constraint is related to the concentration points. We investigate numerically some features of these concentration points such as their weights and their numbers. We show analytically how the constrained Hamilton-Jacobi gives the so-called canonical equation relating their motion with the selection gradient. We illustrate this point numerically.

Key words: adaptive evolution, Turing instability, nonlocal Fisher equation, Dirac concentrations, Hamilton-Jacobi equation.
AMS subject classification: 35K57, 35B25, 49L25, 92C15, 92D15

[1]Corresponding author. E-mail: genieys@math.univ-lyon1.fr

Article available at http://www.mmnp-journal.org or http://dx.doi.org/10.1051/mmnp:2008029

1. Introduction

We consider the periodic solution n to the nonlocal Fisher equation

$$\begin{cases} \dfrac{\partial n}{\partial t} = d\dfrac{\partial^2 n}{\partial x^2} + n\ (1 - \Phi * n), \qquad 0 \le x \le 1, \\ \\ n(t,0) = n(t,1), \qquad \dfrac{\partial n}{\partial x}(t,0) = \dfrac{\partial n}{\partial x}(t,1), \\ \\ n(t=0,x) = n^0 \ge 0, \end{cases} \tag{1.1}$$

where the convolution kernel Φ satisfies

$$\Phi \ge 0, \qquad \int \Phi = 1, \qquad \Phi(x) = 0, \ \text{ for } \ x \notin [-b,b] \quad (b < \frac{1}{2}). \tag{1.2}$$

This is a competition model investigated e.g. by Génieys, Volpert and Auger in [1]. The authors interpret the variable x as a morphological trait, the diffusion term models mutations and the convolution term mimics competition for resources between individuals whose traits are close enough. This type of model is also called "competitive Lotka-Volterra model" in some recent works, [2, 3, 4].

Two length scales can be identified in this model: d for the activation and b for the inhibition. The case $d << b$, *short range activation and long range inhibition*, is typical of Turing's instability [5, 6]. In this regime, we expect pattern formations. This arises from an instability that occurs indeed for certain competition kernels Φ characterized by the fact that their Fourier transform is 'negative enough', as proved in [1, 7, 3] (see also Section A1.). Even though Turing's instability, and thus pattern formation, are more traditional for systems of parabolic PDEs, notice that convolution models are also commonly used in this area, [8, 9]. Is is shown in [1] that in the context of adaptive evolution, the pattern capacity can also lead to an "evolutionary branching": a monomorphic population (i.e. an initial data with a single Dirac mass) may become dimorphic in order to lower the competition. The idea of branching due to the competition can be traced back to Darwin [10] where it is called "divergence principle". It is illustrated numerically with the cellular automata approach in [11], and mathematically investigated by using differential systems in [12, 13, 14, 2]), a probabilistic approach in [15] and game theory in [16].

In the other regime, $b << d$, *long rang activation and short range inhibition* we expect front propagation. Indeed, as $b \to 0$ we recover the classical (local) Fisher equation which is well known to exhibit a travelling wave (see [17, 18] for instance). In this regime, nonlocal Fisher equations were also introduced in ecology for redistributed resources, see [19] and the references therein. Here the questions are the existence of travelling waves in the nonlocal case [20], or of pulsating waves [21], the stability of the steady state n=1 [22] or the existence of periodic solutions [20].

In the present work, we investigate the first regime (pattern formation), when $d \to 0$. Setting $d = \varepsilon^2$ we also rescale the time as $\tau = t/\varepsilon$. This means that we consider large time and small

mutations. The model is then (abusing notations, the new time variable is still denoted t):

$$\begin{cases} \dfrac{\partial n_\varepsilon}{\partial t} = \varepsilon \dfrac{\partial^2 n_\varepsilon}{\partial x^2} + \dfrac{1}{\varepsilon} n_\varepsilon \, (1 - \Phi * n_\varepsilon), \qquad 0 \le x \le 1, \\ n_\varepsilon(t,0) = n_\varepsilon(t,1), \qquad \dfrac{\partial n_\varepsilon}{\partial x}(t,0) = \dfrac{\partial n_\varepsilon}{\partial x}(t,1), \\ n_\varepsilon(t=0,x) = n_\varepsilon^0 \ge 0. \end{cases} \tag{1.3}$$

In this regime, we expect concentration phenomena, like convergence to a sum of Dirac masses. This is indeed the same asymptotics as in the formalism for adaptive dynamics introduced in [13] and also used in [23, 24, 25], where concentration takes place. A convenient tool for studying this concentration is then to introduce a change of variable similar to the phase in the WKB method, since this new variable is more regular than the original one. At the limit $\varepsilon \to 0$, the new variable is usually the solution of a constrained Hamilton-Jacobi equation that allows to study the behavior of the concentration points.

It is the purpose of the present study to perform analytically the Hamilton-Jacobi limit (section 2) and to illustrate it numerically (section 3). We also check numerically that the points where the constraint is saturated are the concentration points, as expected theoretically (section 3). We then investigate numerically some features of the concentration points: their weights and their number. Note that for some particular competition kernels the solution does not tend to a sum of Dirac masses, but rather to a sum of functions with bounded supports (section 3). We then show how the Hamilton-Jacobi equation can be used to obtain the so-called canonical equation relating the velocity of the concentration points to their selection gradient, and illustrate it numerically (section 4). Finally, we summarize our results in the concluding section 5, and gather the technical proofs to the appendix.

2. Hamilton-Jacobi limit

In this section, we recall the method introduced in [13] which allows to analyze the limit $\varepsilon \to 0$ and study the concentration effects. It is based on a classical idea which consists in introducing a 'phase' along with the WKB method for oscillations. Here the parabolic aspect leads us to a real phase as in 'front propagation' analysis introduced in [26, 27].

A simple example that motivates the forthcoming analysis is the 'zero temperature maxwellian' $n_\varepsilon = \frac{1}{\sqrt{2\pi\varepsilon}} e^{-|x|^2/(2\varepsilon)}$. It converges to a Dirac mass at $x = 0$, but it is easier to pass to the limit in the quantity

$$\varepsilon \ln(n_\varepsilon) = \frac{-|x|^2}{2} - \frac{\varepsilon}{2} \ln(2\pi\varepsilon) \xrightarrow[\varepsilon \to 0]{} - \frac{|x|^2}{2} \le 0.$$

With this in mind, we set, following [13, 23, 24],

$$n_\varepsilon(t,x) = e^{\varphi_\varepsilon(t,x)/\varepsilon}, \qquad n_\varepsilon^0(x) = e^{\varphi_\varepsilon^0(x)/\varepsilon}, \tag{2.1}$$

where we assume

$$\varphi_\varepsilon^0(x) \xrightarrow[\varepsilon\to 0]{} \varphi^0(x) \le 0, \qquad \max \varphi^0 = 0.$$

The latter constraint ensures that n_ε^0 neither goes extinct nor blows up in the limit $\varepsilon \to 0$.

Inserting this ansatz in equation (1.3), we find

$$\begin{cases} \dfrac{\partial \varphi_\varepsilon}{\partial t} = \varepsilon \dfrac{\partial^2 \varphi_\varepsilon}{\partial x^2} + \left(\dfrac{\partial \varphi_\varepsilon}{\partial x}\right)^2 + \ (1 - \Phi * n_\varepsilon), \\ \\ \varphi_\varepsilon(t=0,x) = \varphi_\varepsilon^0(x). \end{cases} \tag{2.2}$$

In order to perform the Hamilton-Jacobi limit of equation (2.2) we need a priori estimates on n_ε. We prove that the solution to equation (1.3) has limited growth and non-extinction:

Theorem 1. *Assume (1.2). Then the total mass* $M_\varepsilon(t) = \displaystyle\int_0^1 n_\varepsilon(t,x)dx$ *satisfies*

$$\min\left(M_\varepsilon(0), \frac{1}{\|\Phi\|_\infty}\right) \le M_\varepsilon(t) \le \max\left(M_\varepsilon(0), \frac{1}{\Phi_m c^2}\right),$$

where c *and* Φ_m *are any numbers such that* $\Phi \ge \Phi_m$ *on* $(-2c, 2c)$. *Moreover, as* $t \to \infty$,

$$\liminf M_\varepsilon(t) \ge \frac{1}{\|\Phi\|_\infty}, \qquad \limsup M_\varepsilon(t) \le \frac{1}{\Phi_m c^2}.$$

The proof is in the appendix.

With these estimates on n_ε we obtain an estimate on φ_ε, perform the limit, and obtain a constrained Hamilton-Jacobi equation:

Theorem 2. *We assume (1.2),* $\Phi \in W^{1,\infty}(\mathbb{R})$, $M_\varepsilon(0) = M_0 < \infty$, *and that* φ_ε^0 *and* $\frac{\partial \varphi_\varepsilon^0}{\partial x}$ *are bounded. Then, for all time* $t > 0$, *the solution to equation (2.2) satisfies the a priori bounds*

$$\|\varphi_\varepsilon(t,\cdot)\|_\infty + \left\|\frac{\partial \varphi_\varepsilon}{\partial x}(t,\cdot)\right\|_\infty \le C(t),$$

and, after extraction of a subsequence, $\varphi_\varepsilon \to \varphi \in W^{1,\infty}\big((0,T)\times(0,1)\big)$ *(uniformly locally in time) where* φ *is a solution in the viscosity sense to the Hamilton-Jacobi equation*

$$\begin{cases} \dfrac{\partial \varphi}{\partial t} = \left(\dfrac{\partial \varphi}{\partial x}\right)^2 + r(t,x), \\ \\ \varphi(t=0,x) = \varphi^0(x), \end{cases} \tag{2.3}$$

with

$$r(t,x) = \lim_{\varepsilon\to 0} \ 1 - \Phi * n_\varepsilon \tag{2.4}$$

and satisfies the constraint

$$\max_x \varphi(t,x) = 0 \qquad \forall t \ge 0. \tag{2.5}$$

The proof is in the appendix.
Remarks:

1. *Regularity*: The solutions of Hamilton-Jacobi equations are not smooth and can not be defined in the strong sense. This is the reason why weak solutions had to be defined. Among them the viscosity solutions of Crandall-Lions are by now commonly accepted for Hamilton-Jacobi equations since they are constructed to satisfy the maximum principle property and allow comparisons of solutions, see [28, 29]. There is a specific difficulty here to perform the limit because the time dependency of r is just L^∞ but this is handled with arguments which are now standard and we refer the reader to [23, 14] for further mathematical analysis of this problem. Also, notice that when $\Phi \in C(\mathbb{R})$ this is a uniform limit and $r(t,\cdot) \in C(0,1)$ (continuous functions) for all times.

2. *Interpretation of the equation*: $(\partial\varphi/\partial x)^2$ is the Hamiltonian associated with the term $\partial^2 n_\varepsilon/\partial x^2$ describing the mutations in equation (1.3). When other mutation terms are considered, such as convolution terms, other Hamiltonians are obtained (see [13, 24, 14]). The term $r(t,x)$ is called the *invasion exponent* and describes how the morphology x can invade a given population. It depends on the population through the convolution with Φ that describes the competition. Its gradient $\partial r/\partial x$ is called the *selection gradient* and the points where it vanishes are the so-called *singular points*.

3. *Interpretation of the constraint*: as can be seen from equation (2.1), if $\varphi(t,x) < 0$, $\lim_{\varepsilon\to 0} n_\varepsilon(t,x) = 0$ and if $\varphi(t,x) = 0$, $\lim_{\varepsilon\to 0} n_\varepsilon(t,x) > 0$. Hence the points where the constraint $\max_x \varphi(t,x) = 0$ is saturated are the points where n_ε concentrates as $\varepsilon \to 0$.

4. *Concentration*: The concentration to a unique Dirac mass is investigated in [4] in a similar model. There it is shown that n_ε converges weakly to a measure of the form $n(t,x) = \rho(t)\ \delta(x - \bar{x}(t))$ where $\rho(t)$ is a weight and $\bar{x}(t)$ is the location of the concentration point. The proof of the convergence to a sum of several Dirac masses is an open question. We will see numerically that it usually happens for the present model. Then, assuming that n_ε converges to $n(t,x) = \sum_{i=1}^I \rho_i(t)\ \delta(x - x_i(t))$, we find in (2.5) and (2.4):

$$\varphi(t, x_i(t)) = 0, \qquad i = 1, ..., I, \tag{2.6}$$

$$r(t,x) = 1 - \sum_{i=1}^{I} \rho_i(t)\ \Phi(x - x_i(t)). \tag{2.7}$$

In this case the weights $\rho_i(t)$ can be interpreted as Lagrange multipliers, i.e., free parameters that adapt the right-hand side of equation (2.3) to this constraint.

3. Numerical simulations

3.1. Illustration of the Hamilton-Jacobi limit

In order to illustrate the Hamilton-Jacobi limit, we have to choose an expression for the competition kernel Φ. As it is shown in [1, 7, 3], the pattern forming capacity of equation (1.3) requires that the Fourier transform of Φ takes negative values. For this reason we used M-shaped competition kernels parameterized as

$$\Phi(x) = \Phi(0)\ (1 + a\frac{|x|}{b})\ \mathbf{1}_{\{|x|\leq b\}}, \qquad \int \Phi = 1, \tag{3.1}$$

for real numbers $a > 0$ and $b > 0$. These unusual kernels can be interpreted as describing situations where interspecific competition is stronger that intraspecific competition.

For these even kernels the solution to equation (2.3) tends to a steady-state as will be explained by the canonical equation for concentration points in Section 4.. We first checked the validity of the Hamilton-Jacobi limit at the steady-state: computing the solution n_ε to equation (1.3) for small ε, we compared $\Phi * n_\varepsilon$ to $1 + \left(\frac{\partial \varphi_\varepsilon}{\partial x}\right)^2$. The comparison is shown in Figure 1. The undershoots in the picture to the right are just computational effects when computing the numerical derivative of φ_ε.

We then checked the interpretation of the constraint: the points where $\varphi = 0$ are the concentration point. This is illustrated in Figure 2.

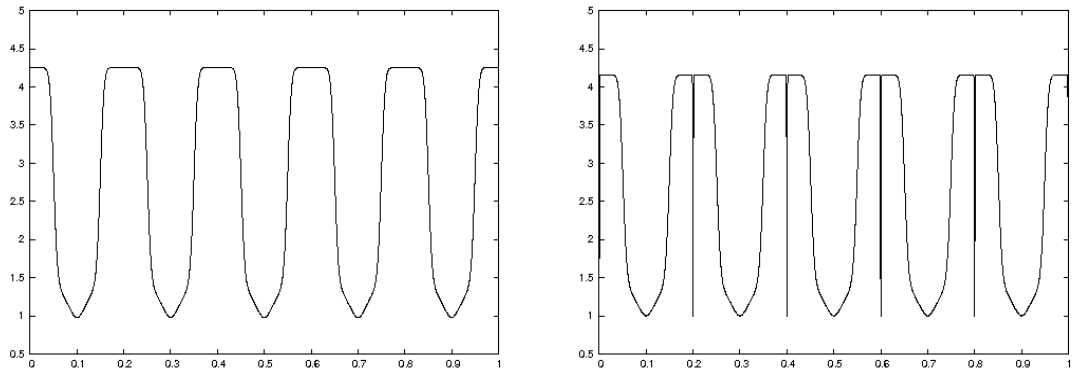

Figure 1: Numerical solution of the problem (1.3) with $\varepsilon = 2.10^{-4}$. The kernel Φ has the M-shape (3.1) with $a = 2$ and $b = 0.15$. We depict the term $\Phi * n_\varepsilon$ (left) and a centered evaluation of $1 + \left(\frac{\partial \varphi_\varepsilon}{\partial x}\right)^2$ (right). The numerics is performed with 3000 points.

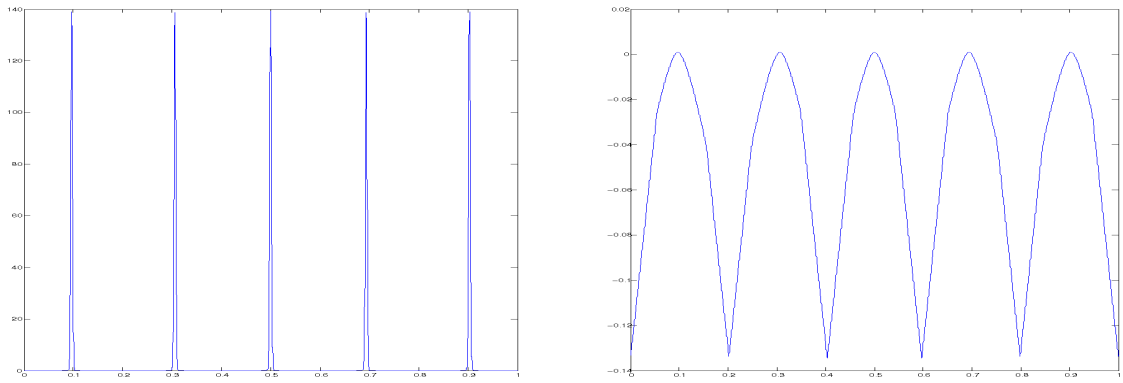

Figure 2: Same as Figure 1. We represent the density n_ε (left) and the phase φ_ε (right).

3.2. Numerical study of concentration patterns

For M-shaped kernels defined by equation (3.1), according to our simulations the steady-state was always a sum of Dirac masses

$$n(x) = \sum_{i=1}^{I} \rho_i \, \delta(x - x_i), \tag{3.2}$$

as exemplified in Figure 2.

Assuming equation (3.2) to hold, according to equation (2.6) the concentration points x_i satisfy $\varphi(t, x_i) = 0$ which yields $\frac{\partial \varphi}{\partial t}(t, x_i) = 0$. Moreover, since the x_i's are maxima of φ, it holds $\frac{\partial \varphi}{\partial x}(t, x_i) = 0$. This implies

$$r(t, x_i) = 0 \qquad 1 \leq i \leq I. \tag{3.3}$$

This equation is standard in the theory of adaptive dynamics, see [13]. We used it to determine the numerically the weights ρ_i. Indeed according to equations (3.2) and (3.3), $0 = r(t, x_i) = 1 - \sum_{j=1}^{I} \rho_j \Phi(x_i - x_j) = 1 - \rho_i \Phi(0)$ if the spacing between the x_i's exceeds the support of Φ.

We checked numerically that the spacing between the concentration point exceeded the support of Φ (not shown) and that the weights ρ_i satisfied $\rho_i = 1/\Phi(0)$. This is illustrated in Table 1. A very good agreement is achieved (to the expense of a very fine grid).

The concentration phenomenon is studied in [4] in a model that is simpler due to the fact that there is a unique concentration point. The convergence to a sum of Dirac masses, in extensions of this model that allow several concentration points, is currently only partially understood. We present here some numerical simulations that give a hint about what can be expected in the model studied in the present paper.

First, the solution might not concentrate to a sum of Dirac masses. According to our simulations, this only happens in the limiting case of kernels (3.1) with $a = 0$ (these kernels hence have a rectangular shape instead of a M shape). In this case, the steady state can be a sum of regular functions with bounded support, centered around evenly spaced points x_i: $n(x) = \sum_{i=1}^{I} u(x - x_i)$. This only happens for very particular initial conditions, that are actually very similar to the ex-

a	$1/\Phi(0)$	numerical weight
0	.3	.300
1	.45	.442
2	.6	.587
3	.75	.724

a	$1/\Phi(0)$	numerical weight
0	.3	.300
1	.45	.447
2	.6	.594
3	.75	.747

Table 1: *Comparison between the predicted values of the weights of the Dirac mass and the weights obtained by numerical simulations. We have taken the parameter* $b = 0.15$ *and left:* $\varepsilon = 2\ 10^{-4}$, 3000 *discretization points, right:* $\varepsilon = 5\ 10^{-5}$, 10000 *discretization points.*

pected steady-state. According to our simulations the spacing between two peaks is the competition scale b. Also, depending on the initial condition, the number of peaks at the steady state may vary. This is exemplified in Figure 3.

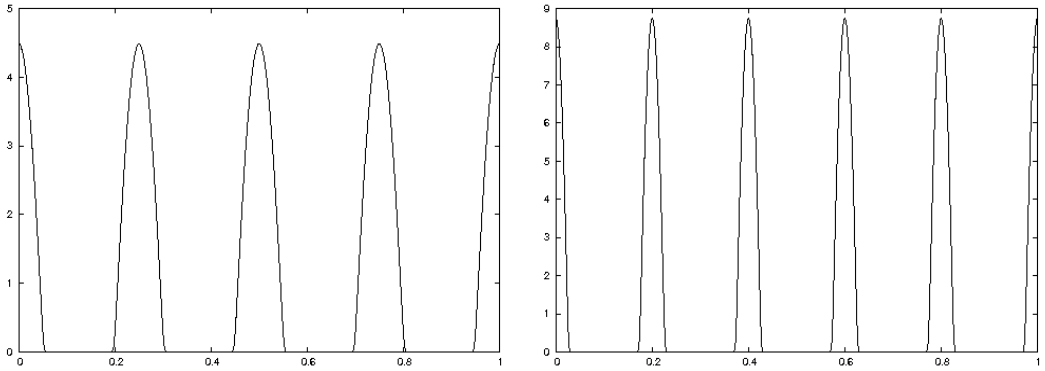

Figure 3: Rectangular kernel defined by (3.1) with $a = 0$ and $b = 0.15$, $\varepsilon = 10^{-4}$. Initial conditions are: 4 peaks evenly spaced (left), 5 peaks evenly spaced (right).

Hence the number of peaks is not known a priori, which might add specific difficulties in the analytical study of the concentration. The same is true for M-shaped competition kernels. In this case, according to our simulations, the solution always concentrates to a sum of Dirac masses, but depending on the initial conditions the number of concentration points may vary. This is shown in Figure 4.

4. Canonical equation for moving concentration points

Assuming that n_ε converges to a sum of Dirac masses $n(t,x) = \sum_{i=1}^{I} \rho_i(t)\ \delta(x - x_i(t))$, where the weights and concentration points now depend on time, we show how the constrained Hamilton-Jacobi equation gives the so-called canonical equation for the motion of the x_i's.

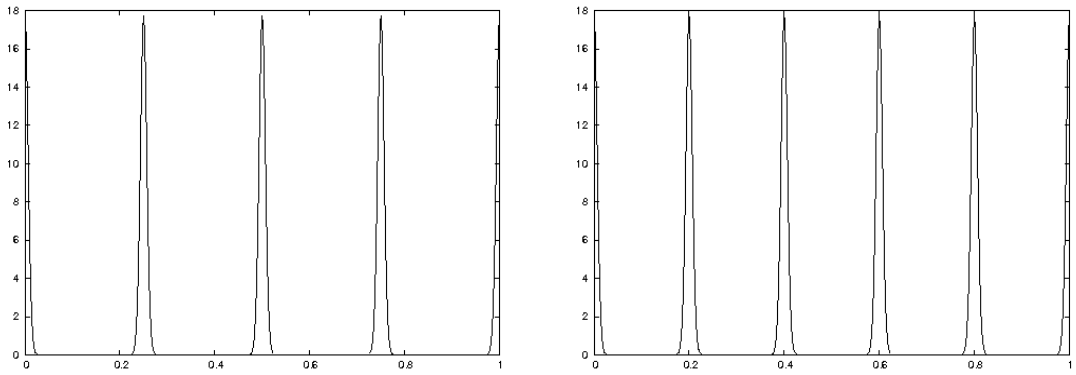

Figure 4: M-shaped kernel (3.1) with $a = 0.015$, $b = 0.15$, $\varepsilon = 10^{-4}$. Initial conditions are: 4 peaks evenly spaced (left), 5 peaks evenly spaced (right).

Following [13, 14], since the concentration points $x_i(t)$ saturate the constraint $\max_x \varphi(t,x) = 0\ \forall t \geq 0$, they satisfy

$$\frac{\partial \varphi}{\partial x}(t, x_i(t)) = 0, \qquad i = 1, ..., I. \tag{4.1}$$

Differentiating equation (4.1) with respect to t gives

$$\frac{\partial^2 \varphi}{\partial t \partial x}(t, x_i(t)) + \dot{x_i}(t) \frac{\partial^2 \varphi}{\partial x^2}(t, x_i(t)) = 0, \tag{4.2}$$

and differentiating equation (2.3) with respect to x,

$$\frac{\partial^2 \varphi}{\partial t \partial x}(t, x_i(t)) = \frac{\partial r}{\partial x}(t, x_i(t)). \tag{4.3}$$

Combining equations (4.2) and (4.3) we obtain the canonical equation for the concentration points, see [13, 14]:

$$\dot{x_i}(t) = \left(-\frac{\partial^2 \varphi}{\partial x^2}(t, x_i(t)) \right)^{-1} \frac{\partial r}{\partial x}(t, x_i(t)). \tag{4.4}$$

This canonical equation can be expressed in terms of Φ. Indeed, according to equation (2.7), the selection gradient satisfies $\frac{\partial r}{\partial x}(t, x_i(t)) = -\sum_{j=1}^{I} \rho_j(t)\ \Phi'(x_i(t) - x_j(t)) = -\rho_i(t)\Phi'(0)$ if the spacing between the x_i's exceeds the support of Φ.

As a consequence, the concentration points move only when $\Phi'(0) \neq 0$. This is the reason why the even kernels of Section 3. lead to steady-state solutions. For asymmetric competition kernels, in this asymptotic, the velocity of the concentration points depends on Φ through the quantity $\Phi'(0)$.

We illustrate this result numerically. We have used the three following kernels

$$\Phi_1(x) = a_1(x + 0.5b)_+\ \mathbf{1}_{\{|x| \leq b\}}, \qquad \int \Phi = 1,$$

$$\Phi_2(x) = a_2(x+b)_+ \ \mathbf{1}_{\{|x|\le b\}}, \qquad \int \Phi = 1,$$

$$\Phi_3(x) = \Phi_3(0)\, \mathbf{1}_{\{-0.5b\le x\le b\}}, \qquad \int \Phi = 1.$$

We have

$$\Phi_1'(0) > \Phi_2'(0) > \Phi_3'(0) = 0,$$

and thus we can expect that the concentration points move faster for Φ_1 than for Φ_2 and that they do not move with Φ_3. This behavior is indeed obtained as depicted in Figure 5.

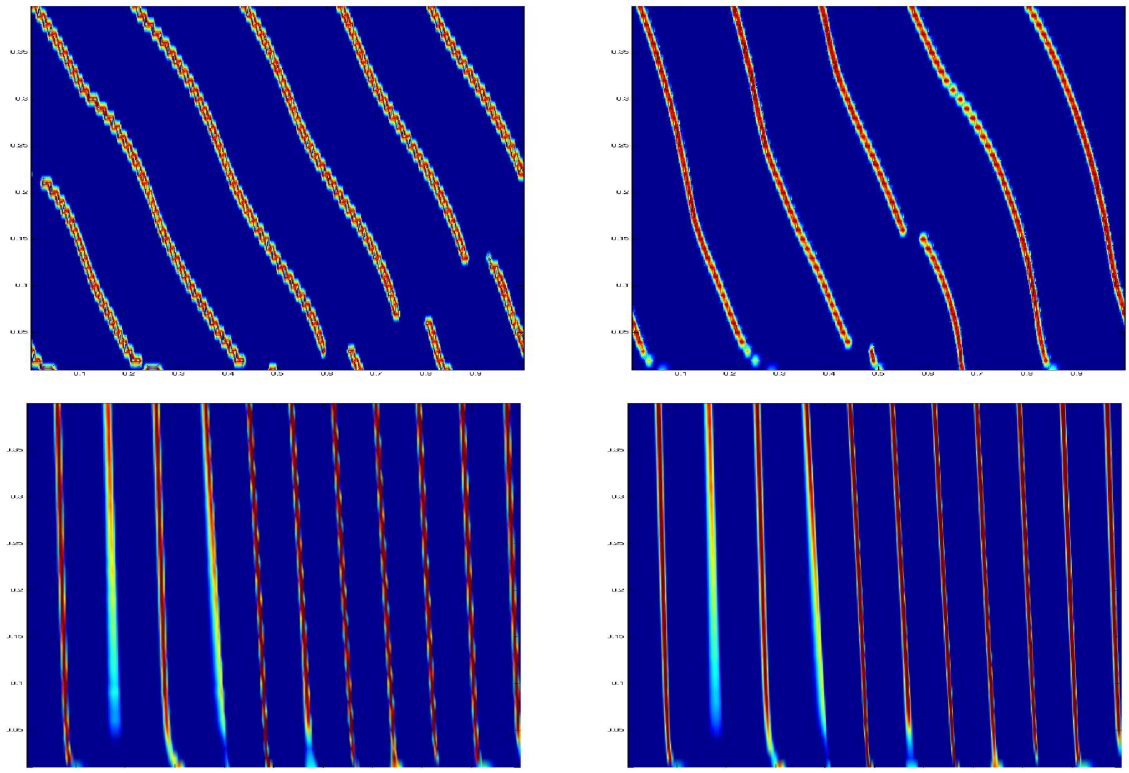

Figure 5: *(Asymmetric competition kernel)* Dynamic of the concentration points with various asymmetric kernels. In the upper left the value $\Phi'(0)$ is larger than in the upper right (a_1 and a_2 respectively). The lower pictures are obtained with an asymmetric kernels satisfying $\Phi'(0) = 0$ (potential Φ_3) with 3000 points on the left and 6000 points on the right. The abscissae are x and the ordinates are time.

5. Conclusion

Following other formalisms for adaptive dynamics [13, 23, 24, 14] it is expected that the scaling introduced in equation (1.3) will produce concentration phenomena. A convenient tool to study the

concentration patterns is to introduce a new variable similar to the phase in the WKB method. This new variable usually leads to a constrained Hamilton-Jacobi equation that permits to investigate the behavior of the concentration points.

In the present work, we proved analytically the convergence to the constrained Hamilton-Jacobi equation. We showed how the constraint on the new variable permits to locate the concentration points, since they are the point where this constraint is saturated (i.e. the points where the new variable equals 0). We checked the convergence numerically, and that the concentration points indeed saturated the constraint. This was done for unusual competition kernels that were not decreasing with respect to the distance between morphologies (they actually had the shape of a "M"). The reason is that equation (1.3) exhibits pattern-forming capacity only for kernels characterized by the fact that their Fourier transform take negative values. The M-shaped kernels are simple ones that possess this property. We interpreted them as modelling situations where the interspecific competition is larger than the intraspecific one, but we mainly used them as simple profiles allowing us to illustrate the Hamilton-Jacobi method.

We did not prove analytically the convergence of the solution to a sum of Dirac masses. This is done in [4] for a model where there is a unique concentration point, and the case of multiple concentration points is currently an open question. For the model investigated in the present paper, we addressed this question numerically, trying to get some hints about what can be expected. Usually, starting from any initial condition, the solution concentrated to a sum of Dirac masses. But the number of masses was not fixed and depended on the initial condition. The spacing between two masses always exceeded the competition range b. We then checked that the weights of these masses were in accordance with their theoretical value. Only for the particular rectangular competition kernels, and with particular initial conditions, the solution concentrated to a sum of regular functions with bounded (but nonzero) support. The rectangular kernels are of course more usual than the M-shaped ones, but the concentration to a sum of regular functions seems to us "non-generic" in some sense, since it necessitates very particular initial conditions (actually, initial conditions have to already a sum of regular functions).

We finally showed how the constrained Hamilton-Jacobi equation can be used to obtain the so-called canonical equation that describes the motion of the concentration points. It turns out that their velocity is related to the derivative of the competition kernel at the origin, explaining why symmetric kernels lead to steady-state solutions and asymmetric kernels to moving concentration points.

A Mathematical proofs and numerical algorithms

In this section we gather several mathematical results that have been used throughout the paper. They mostly concern a priori estimates. We also describe, for the sake of completeness, the numerical algorithms that we have used.

A1. Turing's instability and estimation of the typical wave length

For the sake of completeness we reproduce here the computation for deriving the Turing instability condition in model (1.3), following [1].

Linearizing the equation (1.3) around the steady state $n = 1$, we obtain

$$\begin{cases} \dfrac{\partial r}{\partial t} - \varepsilon \dfrac{\partial^2 r}{\partial x^2} = -\dfrac{1}{\varepsilon} \Phi * r, \qquad 0 \le x \le 1, \\ \\ r(t,\cdot) \ \text{1-periodic.} \end{cases}$$

As usual one tries to find solutions with exponential growth, which means eigenvectors

$$\begin{cases} \lambda r(x) - \varepsilon \dfrac{\partial^2 r}{\partial x^2} = -\dfrac{1}{\varepsilon} \Phi * r, \qquad 0 \le x \le 1, \\ \\ r(\cdot) \ \text{1-periodic}, \qquad \lambda > 0. \end{cases} \tag{A1}$$

It is natural to decompose a possible solution r in Fourier series

$$r(x) = \sum_{n \in \mathbb{Z}} \widehat{r}(n) e^{2i\pi n x}, \qquad \widehat{r}(n) = \int_0^1 r(x) e^{-2i\pi n x} dx.$$

Then, equation (A1) becomes

$$\widehat{r}(n) \big[\lambda + \varepsilon (2\pi n)^2 + \frac{1}{\varepsilon} \widehat{\Phi}(n) \big] = 0.$$

Consequently, the eigenvalues are given by

$$\lambda = -\varepsilon (2\pi n)^2 - \frac{1}{\varepsilon} \widehat{\Phi}(n). \tag{A2}$$

Turing instability occurs when some Fourier coefficient of Φ is negative and the leading positive eigenvalue is given for ε small, by

$$\lambda_\varepsilon \approx -\frac{1}{\varepsilon} \min_n \widehat{\Phi}(n) = -\frac{1}{\varepsilon} \widehat{\Phi}(n_0).$$

The corresponding eigenvector is $e^{2i\pi n_0 x}$, which exhibits a wave length $L_0 = \frac{1}{|n_0|}$.

We can specify the example $\Phi = \frac{1}{2b} \mathbf{1}_{\{|x| \le b\}}$, with $b < \frac{1}{2}$ and we find that

$$\widehat{\Phi}(n) = \frac{1}{2b} \int_{-b}^{b} e^{-2i\pi n x} dx = \frac{1}{2\pi n b} \sin(2\pi n b).$$

The smallest frequency such that instability occurs, $\widehat{\Phi}(n_0) = 0$, is given here by $n_0 = E(\frac{1}{2b}) + 1$, where E is the "integer part" function, and thus $L_0 = 1/[E(\frac{1}{2b}) + 1]$ (which is close to $2b$ when b is small). This is also the largest possible length of patterns but in practice a different wave length may be obtained depending on the initial conditions (see subsection 3.2.).

A2. Mass control for the nonlocal Fisher equation

Proof of Theorem 1. (i) Non-extinction. Integrating in x the equation (1.3), we obtain the relation

$$\frac{d}{dt}M_\varepsilon(t) = \frac{1}{\varepsilon}\left(M_\varepsilon(t) - \int_0^1 n_\varepsilon\ \Phi * n_\varepsilon dx\right), \tag{A3}$$

and we have

$$\int_0^1 n_\varepsilon \Phi * n_\varepsilon dx \le \|\Phi\|_\infty\ M_\varepsilon^2(t).$$

Therefore, since $n_\varepsilon \ge 0$, we arrive to the differential inequality

$$\frac{d}{dt}M_\varepsilon(t) \ge \frac{M_\varepsilon(t)}{\varepsilon}\left(1 - M_\varepsilon(t)\|\Phi\|_\infty\right),$$

which proves the lower bound.

(ii) Limited growth. Consider a value $c > 0$ as in the statement of Theorem 1, and an interval I of length c where

$$\int_I n_\varepsilon dx \ge c\ M_\varepsilon(t).$$

Then, still with the notations in the statement of Theorem 1, we have the lower bounds

$$\begin{aligned}\int_0^1 n_\varepsilon\ \Phi * n_\varepsilon dx &\ge \Phi_m \int_{|x-y|\le 2c} n_\varepsilon(t,x)\ n_\varepsilon(t,y)\ dxdy \\ &\ge \Phi_m \int_{I\times I} n_\varepsilon(t,x)\ n_\varepsilon(t,y)\ dxdy \\ &\ge \Phi_m c^2 M_\varepsilon^2(t).\end{aligned}$$

Therefore, we obtain from (A3)

$$\frac{d}{dt}M_\varepsilon(t) \le \frac{M_\varepsilon(t)}{\varepsilon}\left(1 - c^2 M_\varepsilon(t)\Phi_m\right),$$

and again the upper bound follows directly. □

A3. Estimates for the Hamilton-Jacobi equation

Proof of Theorem 2. Differentiating equation (2.2) with respect to x, we obtain the equation for $w = \dfrac{\partial \varphi_\varepsilon}{\partial x}$,

$$\frac{\partial w}{\partial t} = \varepsilon\frac{\partial^2 w}{\partial x^2} + 2\frac{\partial \varphi_\varepsilon}{\partial x}\cdot\frac{\partial w}{\partial x} - \Phi' * n_\varepsilon. \tag{A4}$$

Here, we can upper bound

$$|\Phi' * n_\varepsilon(t)| \leq \|\Phi'\|_\infty \bar{M}(t),$$

where $\bar{M}(t)$ is an upper bound of the total mass $M(s)$ for times $0 \leq s \leq t$ which is controlled thanks to Theorem 1. Therefore, by the maximum principle, we have

$$|w(t,x)| \leq \max_{x\in(0,1)} |w(t=0,x)| + \|\Phi'\|_\infty \bar{M}(t)t.$$

This uniform estimate on the gradient gives a uniform estimate on φ_ε in $L^\infty\big((0,T)\times(0,1)\big)$ when coming back to the equation (2.2) because it boils down to the heat equation with a bounded right-hand side. And thus, the L^∞ bounds on φ_ε and $\frac{\partial\varphi_\varepsilon}{\partial t}$, as stated in Theorem 2, are proved.

Then we can obtain a local uniform L^2 estimate on $\frac{\partial\varphi_\varepsilon}{\partial t}$. To do that, we multiply for instance the equation (2.2) by $\frac{\partial\varphi_\varepsilon}{\partial t}$, and integrate. We obtain, denoting by C an absolute bound for $\left(\frac{\partial\varphi_\varepsilon}{\partial x}\right)^2 + 1 - \Phi * n_\varepsilon$

$$\begin{aligned}\int_0^1 \left(\frac{\partial\varphi_\varepsilon}{\partial t}\right)^2 dx &\leq \varepsilon \int_0^1 \frac{\partial\varphi_\varepsilon}{\partial t}\frac{\partial^2\varphi_\varepsilon}{\partial x^2} dx + C\int_0^1 \left|\frac{\partial\varphi_\varepsilon}{\partial t}\right| dx \\ &\leq -\frac{\varepsilon}{2}\frac{d}{dt}\int_0^1 \left(\frac{\partial\varphi_\varepsilon}{\partial x}\right)^2 dx + C\int_0^1 \left|\frac{\partial\varphi_\varepsilon}{\partial t}\right| dx.\end{aligned}$$

Therefore, when integrating in time and using Cauchy-Schwarz inequality for the second term on the right, we find

$$\int_0^T\int_0^1 \left(\frac{\partial\varphi_\varepsilon}{\partial t}\right)^2 dxdt \leq \frac{\varepsilon}{2}\int_0^1 \left(\frac{\partial\varphi_\varepsilon}{\partial x}(t=0)\right)^2 dx + C\sqrt{T}\left(\int_0^T\int_0^1 \left(\frac{\partial\varphi_\varepsilon}{\partial t}\right)^2 dxdt\right)^{1/2}.$$

This proves a uniform bound on the quantity $\displaystyle\int_0^T\int_0^1 \left(\frac{\partial\varphi_\varepsilon}{\partial t}\right)^2 dxdt$. Together with the bound on the x derivative, this proves the compactness of φ_ε for the uniform topology.

Passing to the limit in viscosity sense and almost everywhere is standard then. The constraint $\max\varphi(t,\cdot) = 0$ follows from the mass constraint (see [13, 23, 14]). Indeed, would this max be negative, then n_e would go extinct which is not true; would this max be positive, then by continuity this would be true in an interval and n_e would blow up, contradicting the finite mass property. □

A4. Numerical methods

We have used two different numerical schemes that we describe now. Both of them are very simple and based on finite differences.

In the first scheme, the discretization of equation (1.1) is based on a time splitting of the reaction term $n(1-\Phi*n)$ and the differential term. Considering a number N of points in x, we approximate

the solution by a discrete vector n_i^k for $i = 1, ..., N$ and k the label for discrete time. We set $\Delta x = 1/N$ the space stepping and Δt the time stepping.

In order to avoid strong limitations on the time step, we use an exact resolution of the reaction term

$$n_i^{k+1/2} = n_i^k \exp\big(\frac{\Delta t}{\varepsilon}(1 - \Phi * n^k)\big),$$

where the convolution $\Phi * n$ is computed according to

$$\Phi * n \approx \frac{1}{N} \sum_{j=-J_M}^{J_M} \Phi_j n_{i-j},$$

where $J_M = b * N$. We use a three point implicit (or explicit when ε is small enough) scheme for the differential term

$$n_i^{k+1} = n_i^{k+1/2} + \frac{\varepsilon\ \Delta t}{2\Delta x^2}\ [n_{i+1}^{k+1} + n_{i-1}^{k+1} - 2n_i^{k+1}].$$

In the second scheme, we use an explicit scheme for the reaction as well as for the diffusion. The convolution is computed by using the trapeze formula:

$$\Phi * n \approx \frac{1}{N} \sum_{j=0}^{J_M-1} (\Phi_j n_{i-j} + \Phi_{j+1} n_{i-j-1})/2 + (\Phi_{-j} n_{i+j} + \Phi_{-j-1} n_{i+j+1})/2.$$

This gives a better accuracy and allows to check that the number of discretization points is enough to resolve the singularities.

Finally, notice that for accuracy reasons it is necessary to ensure some kind of CFL condition

$$\frac{\Delta t}{\varepsilon} \ll 1. \tag{A5}$$

This is imposed in order to ensure that the reaction term is well resolved. In practice we can choose $\frac{\Delta t}{\varepsilon} = .1$. As a consequence, when ε is small, the CFL condition for the diffusion term, namely

$$\frac{\varepsilon\ \Delta t}{2\Delta x^2} \leq 1,$$

can be achieved. Then the explicit scheme for the diffusion is stable.

References

[1] S. Génieys, V. Volpert, P. Auger, *Pattern and waves for a model in population dynamics with nonlocal consumption of resources.* Math. Model. Nat. Phen., 1 (2006), No. 1, 65-82.

[2] G. Meszena, M. Gyllenberg, F. J. Jacobs, J. A. J. Metz, *Link between population dynamics and dynamics of Darwinian evolution.* Phys. Rev. Lett., 95 (2005), 078105.

[3] S. Pigolotti, C. Lopez, E. Hernandez-Garcia, *Species clustering in competitive Lotka-Volterra models.* Phys. Rev. Lett., 98 (2007), 258101.

[4] B. Perthame, G. Barles, *Dirac concentrations in Lotka-Volterra parabolic PDEs.* http://hal.archives-ouvertes.fr/hal-00168404/fr/, Preprint, (2007).

[5] A. M. Turing, *The chemical basis of morphogenesis.* Phil. Trans. Roy. Soc. B, 237 (1952), 37-72.

[6] H. Meinhardt. Models of biological pattern formation. Academic Press, London, 1982.

[7] M. A. Fuentes, M. N. Kuperman, V. M. Kenkre, *Analytical considerations in the study of spatial patterns arising from nonlocal interaction effects.* J. Phys. Chem. B, 108 (2004), 10505-10508.

[8] R. Lefever, O. Lejeune, *On the origin of tiger bush.* Bull. Math. Biology, 59 (1997), No. 2, 263-294.

[9] L. Desvillettes, C. Prevost, R. Ferrière, *Infinite Dimensional Reaction-Diffusion for Population Dynamics.* Preprint n. 2003-04 du CMLA, ENS Cachan.

[10] C. Darwin. On the origin of species by means of natural selection. John Murray, London, 1859.

[11] S. Atamas, *Self-organization in computer simulated selective systems.* Biosystems, 39 (1996), 143-151.

[12] S. A. H. Geritz, E. Kisdi, G. Meszena, J. A. J. Metz, *Evolutionary singular strategies and the adaptive growth and branching of the evolutionary tree.* Evol. Ecol., 12 (1998), 35-57.

[13] O. Diekmann, P.-E. Jabin, S. Mischler, B. Perthame, *The dynamics of adaptation: an illuminating example and a Hamilton-Jacobi approach.* Th. Pop. Biol., 67 (2005), No. 4, 257-271.

[14] B. Perthame. Transport equations in biology. Series 'Frontiers in Mathematics', Birkhauser, 2006.

[15] N. Champagnat, R. Ferrière, S. Méleard, *Unifying evolutionary dynamics: from individual stochastic processes to macroscopic models.* Th. Pop. Biol., 69 (2006), No. 3, 297-321.

[16] J. Hofbauer, K. Sigmund. Evolutionary games and population dynamics. Cambridge University Press, Cambridge, 1998.

[17] J. D. Murray. Mathematical biology, Vol. 1 and 2, Second edition, Springer, 2002.

[18] H. Berestycki, F. Hamel. Reaction-Diffusion Equations and Propagation Phenomena. Series Appl. Math. Sci., Springer, 2006.

[19] S. A. Gourley, *Travelling front of a nonlocal Fisher equation.* J. Math. Biol., 41 (2000), 272-284.

[20] Z.-C. Wang, W.-T. Li, S. Ruan, *Travelling Wave Fronts in Reaction-Diffusion Systems with Spatio-Temporal Delays.* J. Differential Equations, 222 (2006), No. 1, 185-232.

[21] H. Berestycki, F. Hamel, N. Nadirashvili, *The speed of propagation for KPP type problems. I. Periodic framework.* J. Eur. Math. Soc., 7 (2005), No. 2, 173-213.

[22] H. Berestycki, G. Nadin, B. Perthame, L. Ryzhik, Work in preparation.

[23] G. Barles, B. Perthame, *Concentrations and constrained Hamilton-Jacobi equations arising in adaptive dynamics.* In Recent Developments in Nonlinear Partial Differential Equations, D. Danielli editor. To appear in Contemp. Math. (2007).

[24] J. A. Carrillo, S. Cuadrado, B. Perthame, *Adaptive dynamics via Hamilton-Jacobi approach and entropy methods for a juvenile-adult model.* Mathematical Biosciences, 207 (2007), No. 1, 137-161.

[25] L. Desvillettes, P.-E. Jabin, S. Mischler, G. Raoul, *On mutation selection dynamics.* Preprint (2007).

[26] L. C. Evans, P. E. Souganidis, *A PDE approach to geometric optics for certain semilinear parabolic equations.* Indiana Univ. Math. J., 38 (1989), 141-172.

[27] G. Barles, L. C. Evans, P. E. Souganidis, *Wavefront propagation for reaction diffusion systems of PDE.* Duke Math. J., 61 (1990), 835-858.

[28] M. G. Crandall, H. Ishii, P.-L. Lions, *User's guide to viscosity solutions of second order partial differential equations.* Bull. Amer. Math. Soc., **27** (1992), 1-67.

[29] W. H. Fleming, H. M. Soner. Controlled Markov processes and viscosity solutions. Applications of Mathematics 25, Springer, 1993.